



HAL
open science

Cretaceous paleomargin tilted blocks geometry in Northern Tunisia: stratigraphic consideration and fault kinematic analysis

Chahreddine NAJI

Chahreddine Naji, Amara Masrouhi, Zayneb Amri, Mohamed Gharbi, Olivier Bellier

► To cite this version:

Chahreddine Naji, Amara Masrouhi, Zayneb Amri, Mohamed Gharbi, Olivier Bellier. Cretaceous paleomargin tilted blocks geometry in Northern Tunisia: stratigraphic consideration and fault kinematic analysis Chahreddine NAJI. *Arabian Journal of Geosciences*, 2018, 11 (19), pp.583. 10.1007/s12517-018-3930-7 . hal-01892586

HAL Id: hal-01892586

<https://hal.science/hal-01892586v1>

Submitted on 10 Oct 2018

HAL is a multi-disciplinary open access archive for the deposit and dissemination of scientific research documents, whether they are published or not. The documents may come from teaching and research institutions in France or abroad, or from public or private research centers.

L'archive ouverte pluridisciplinaire **HAL**, est destinée au dépôt et à la diffusion de documents scientifiques de niveau recherche, publiés ou non, émanant des établissements d'enseignement et de recherche français ou étrangers, des laboratoires publics ou privés.

Cretaceous paleomargin tilted blocks geometry in Northern Tunisia: stratigraphic consideration and fault kinematic analysis

Chahreddine NAJI ^{a,b,*}, Amara MASROUHI ^c, Zayneb AMRI ^{a,b}, Mohamed GHARBI ^a, Olivier BELLIER ^d

^a *Geo-Resources Laboratory, Water Researches and Technologies Center Borj-Cedria, Soliman, Tunisia*

^b *Université de Carthage, Faculté des Sciences de Bizerte, Bizerte, Tunisia*

^c *King Abdulaziz University, Faculty of Earth Sciences, Geo-exploration Techniques Department, Jeddah, Saudi Arabia*

^d *Aix Marseille Univ, CNRS, IRD, Coll France, CEREGE, Aix-en-Provence, France*

* Corresponding author: chahreddine.naji.geo@gmail.com

Abstract:

New stratigraphic data, lithostratigraphic correlations and fault kinematic analysis are used to discuss the basin geometry and sedimentation patterns of the northeastern Tunisia during Cretaceous times. Significant facies and thickness variations are deduced along the northeastern Atlas of Tunisia. The NW-SE 80 km-long regional correlation suggests a high sedimentation rates associated with irregular sea floor. The fault kinematic analysis highlights N-S to NE-SW tectonic extension during early Cretaceous. During Aptian-Albian times, an extensional regime is recognized with NE-SW tectonic extension. The Cenomanian-Turonian fault populations highlight a WNW-ESE to NW-SE extension, and, Campanian-Maastrichtian faults illustrate NW-SE extension. The normal faulting is associated to repetitive local depocenters with a high rate of sedimentation as well as abundant syntectonic conglomeratic horizons, slump folds and halokinetic structures. The sequences correlation shows repetitive local depocenters characterizing the basin during early Cretaceous times. All the above arguments are in favor of basin configuration with tilted blocks geometry. This geometry is shaped by major synsedimentary intra-basin listric normal faults, themselves related to the extensional setting of the southern Tethyan paleomargin, which persisted into the Campanian-Maastrichtian times. The results support a predominant relationship between tilted blocks geometry and sedimentation rather than E-W "Tunisian Through" as it was previously accepted.

Keywords: Cretaceous, tilted blocks, stratigraphic consideration, fault kinematic, Tunisia.

30 Introduction

31 The present-day structure of the Northern African margin in Tunisia results from a complex tectonic
32 evolution that operated since late Permian with the beginning of the breakup of Pangea and ended
33 with the Cenozoic Alpine orogeny of the Maghrebide chain. The geodynamic evolution of the
34 northern margin of Africa has been characterized by extension, crustal stretching and thinning, as
35 well as subsidence during the Mesozoic Tethyan rifting (Boughdiri et al., 2007; Gharbi et al., 2013; El
36 Amari et al., 2016; Soussi et al. 2017, Naji et al., 2018). The Mesozoic passive margin, where rifting
37 occurred, was followed by subsequent inversion during Late Cretaceous-Cenozoic subduction and
38 ended by Alpine collisional process (De Lamotte et al., 2009; Khomsi et al., 2016). During the Jurassic
39 time, a regional extensional tectonic regime produced the dislocation of the existing continental
40 platform, which is related to the opening of the Central Atlantic and led to the development of
41 normal faults, tilted blocks and Halokinetic and volcanic activity (Mattoussi Kort et al., 2009;
42 Masrouhi et al., 2014a; Dhahri and Boukadi, 2017). The Tunisian Atlas has particularly recorded the
43 effect of Tethyan rifting as revealed by considerable facies and thickness variations within the
44 Mesozoic sequences (Ben Ferjani et al., 1990; Masrouhi and koyi, 2012; Gharbi et al., 2015; El Amari
45 et al., 2016). The complex structural pattern of Tunisia is mainly a consequence of the polyphased
46 Cenozoic reactivation of inherited extensional faults systems which controlled fault-related folds
47 (Masrouhi et al., 2008; Dhahri and Boukadi, 2010; Gharbi et al., 2015; Khomsi et al., 2016).

48 The present study focuses on the basin geometry and sedimentation patterns of northeastern
49 Tunisia during Cretaceous times. In this study, new sedimentologic, stratigraphic, paleontologic and
50 structural data are reported to understand the basin configuration of the southern Tethyan
51 paleomargin in northern Tunisia. This work aims to contribute to the debate about the basin
52 paleogeography during Mesozoic times on the basis of structural field data, stratigraphic precisions,
53 lithostratigraphic correlations and fault kinematic analysis.

54 1. Geologic setting

55 The northern Tunisian belt forms the northeastern edge of the African plate and set the eastern
56 limits of the Atlas System. Except its northerly range which corresponds to the Numidian thrust
57 Range, the Northern Tunisian Atlas is classically subdivided into two distinguished structural units
58 (Fig. 1a): The first unit corresponds to the southeastward major thrust unit called the Teboursouk
59 thrust unit which represents the front of the Alpine Range. This area shows thick Aptian–Albian
60 sequences and exhibits frequent outcropping salt structures belonging to the northeastern Maghreb
61 salt province (Masrouhi et al, 2013; Jaillard et al., 2017). The second one called the Zaghouan-Ressas
62 unit corresponds to the front of the northern Tunisian Alpine Range. During Mesozoic times, the
63 present Zaghouan Thrust Fault corresponds to a paleogeographic line between a relatively shallow

64 platform to the south, with a condensed Aptian section from a deep basin to the north with a thick
65 Aptian–Albian section (Morgan et al., 1998; Chihaoui et al., 2010; Soua, 2016).

66 The Meso–Cenozoic geological evolution of the northern African margin can be summarized in two
67 main periods. The first period, from the late Permian? To the early Cretaceous, of the Mesozoic
68 rifting is related to the Tethyan and Atlantic Oceans opening (Guiraud, 1998). Recent works
69 demonstrate that the opening of Central Atlantic operates during Jurassic and early Cretaceous
70 (Souquet et al., 1997; Boughdiri et al., 2007; Masrouhi and Koyi, 2012; Naji et al., 2018).
71 Furthermore, related Cretaceous salt movement confirms a hyperactive extension, thick and/or thin-
72 skinned tectonic extension (Masrouhi et al., 2014b). In addition, frequent synsedimentary normal
73 faults are recognized to produce a general tilted-blocks geometry. During this period, the Aptian–
74 Albian ages are described to have developed syndepositional facies and thickness heterogeneities of
75 the south Tethyan margin in north Tunisia (Souquet et al., 1997; Gharbi et al., 2013; Masrouhi et al.,
76 2014b; Naji et al., 2018). Commonly, the Cretaceous sequences, outcropping in northern Tunisia,
77 display significant thickness and/or facies variations with abundant soft-sediment deformations and
78 syntectonic growth strata (Gharbi et al., 2013; Naji et al., 2018).

79 The second main period, started since Late Cretaceous (at Campanian-Maastrichtian transition),
80 causes a basin positive inversion related to the African and Eurasian plate convergence (Guiraud and
81 Bosworth, 1997; Khomsi et al., 2009; Gharbi et al., 2015; El Amari et al., 2016).

82 2. Lithostratigraphy of early Cretaceous successions

83 2.1. Jebel Sidi Salem section

84 The Sidi Salem–Messella is a NE-trending structure located along the Zaghouan–Ressas thrust system
85 (Fig. 1b). The early Cretaceous outcropping in this structure includes sequences ranged from
86 Neocomian to Albian (Fig. 2). The outcropping Cretaceous sequences are subdivided as follows:

- 87 a- A first unit consists of marls –to- marly limestone succession, which are attributed to the
88 Neocomian without additional precision (Fig. 2). These units, include pelagic and benthic
89 fauna, indicate deposit of a marine environment.
- 90 b- The Neocomian deposits are covered by gray marls interbedded with quartzitic and clayey
91 limestone beds with ammonites at the base and topped by dark marls. This ~150 m-thick unit
92 of clayey facies delivered a faunal assemblage dominated by benthic foraminifera
93 *Lenticulina*, *Nodosaria* and *Dentalina* (Elkhazri et al., 2009; confirmed by M. Ben Youssef)
94 which indicated the Barremian age.
- 95 c- Green to Gray laminated marls intercalated with sandstones and gray nodular limestone
96 beds showing in outcrop abundant Belemnites and Ammonites macrofauna. The common
97 presence of bi-pyramidal quartz indicates halokinesis activity during this period. This ~300 m

98 thick unit is dated as Aptian. Nagazi (2016), with an extensive biostratigraphic analysis, shows
99 that the Jebel Sidi Salem's Aptian sequences are subdivided as follow:

- 100 • Early Aptian (Bedoulian) is dominated by a planktonic association which contains:
101 *Gorbachikella grandiapertura Hedbergella sigali, Schackoïna cabri, Lenticulina*
102 *bizonae* and *L. protuberans* associated with Benthic foraminifera: *Lenticulina*
103 *ouachensis, Gavelinella barremiana, Nodosaria paupercula* and *Gavelinella* sp.
 - 104 • Middle Aptian (Gargasian) is identified by micropaleontological association with:
105 *Globigerinoïdes barri, Globigerinoïdes ferreolensis, Leupoldina protuberans,*
106 *Globigerinelloides algerianus, Globigerinelloides ferreolensis, Hedbergella trocoïda.*
 - 107 • Uppermost Aptian (Clansayesian) is marked by the appearance of *Hedbergella*
108 *trochoïda (Gandolfi), Pseudoplanomalina cheniourensis (Sigal)* and *Hedbergella*
109 *palanispira* associated to benthic foraminifera such as *Gavelinella* sp., *Ammodiscus*
110 *tennuissimus, Trochammina* sp.
 - 111 • Aptian sequences are covered by gray to black marls succession with thin beds of
112 nodular and quartzitic limestone. According to the biostratigraphic analysis of Nagazi
113 (2016), this unit contain the following planktonic foraminifers' assemblage: *Ticinella*
114 *primula, Ticinella bejaouansis, Rotalipora ticinensis, Hedbergella trocoïda, Ticinella*
115 *roberti* and *Rotalipora subticinensis*, which indicate a middle Albian age. The top of
116 the unit is made of marls sequences with platy limestone succession beds which are
117 attributed to the uppermost Albian (Vraconian in literature) on the basis of the
118 following micropaleontological association: *Planomalina buxtorfi, Biticinella*
119 *breggiensis, Rotalipora appenninica, Dentalina guttifera* and *Praedorothia hechti,*
120 *subticinensis R.,* and *B. ticinensis breggeinsis*. The 180 m-thick Albian sequences
121 contain abundant black shale levels, testifying for deep sea environment deposition.
122 The Albian strata are characterized by abundant slumps and carbonate nodules
123 symptomatic of contemporaneous sub-marine slope.
- 124 d- 120 m-thick series made of nodular limestone interbedded by marls dated as early
125 Cenomanian. The top of these monotone sequences is marked by thinly laminated, dark-grey
126 limestone and marl of the uppermost Cenomanian-early Turonian-aged Bahloul Member.
- 127 e- Coniacian–Santonian-aged sequences of the Aleg Formation conformably overlie the
128 previous Cenomanian-Turonian series. They are defined by thick sequences of limestone
129 interbedded with marl layers at the base and thick marly sequences at the top. The
130 Coniacian–Santonian series can reach a maximum ~450 m in thickness in the northern flank

131 of Sidi Salem anticline. These sequences are topped by the Campanian-Maastrichtian Abiod
132 Formation with three well-known terms.

133 **2.2. Jebel Oust type-section**

134 The Jebel Oust is a 15 km-large N40°E-trending anticline structure exposes series ranging from
135 Jurassic sequences in the core and Campanian–Maastrichtian outcrops in the limbs. In this locality,
136 which is considered in northern Tunisia as the type-section of lower Cretaceous (Ben Ferjani et al.,
137 1990; Souquet et al., 1997), 2600 m-thick siliciclastic and marly sequences (Fig. 3) have been
138 deposited (Fig. 3). According to Souquet et al. (1997), this “reference section” is made of:

139 a- 90 m of debris flow deposits and marl calpionellid bearing mudstone parasequences which
140 correspond to the Tithonian-Berriasian transition followed by mud-flow and debris flow
141 deposits of 40 m-thick which marked the early Berriasian. The Berriasian *p.p* is made of ~160
142 m of greenish muds with thin bedded sandstones and siltstones. The following
143 micropaleontological association was described by Maamouri and Salaj (1978): *Tintinopsella*
144 *carpathica*, *Spirillina neocomiana*, *Trocholina infragranulata* North, *Trocholina vasserodi*
145 Guillaume, *Trocholina molesta* Gorbastschek, *Trocholina burlini* Gorbastschek, *Spirillina*
146 *neocomiana* Moullade and *Spirillina minima* Schacko. These units are covered by a 160 m
147 carbonate dominated sequences which are attributed by souquet al. (1997) to the
148 uppermost Berriasian–early Valanginian.

149 b- A large 900 m-thick unit consists of siliciclastic turbidites with pelites, thin-bedded
150 sandstones, slumped quartzites bed and sometimes sliding blocks which corresponds to
151 Valanginian deposits. This unit is covered by 120 m-thick rich Ammonites mudstones marked
152 by *Castellensis* zone which indicates the lower Hauterivian (Souquet et al., 1997) followed by
153 aggrading marls-mudstone parasequences. To the top, a ~280 m-thick siliciclastic and
154 carbonate storm with marls succession is attributed to the late Hauterivian.

155 c- The Barremian is made up of siliciclastic tempestites and slumped sandstone beds (Fig. 3)
156 followed by thick nodular limestone bar, siliciclastic storm topped by black-shales. This ~600
157 m-thick unit delivered to Maamouri and Salaj (1978) *Anomila (Gavelinella) sigmoicosta*
158 *barremiana*, *Epistomina (Brotzenia) hechti* which indicates the early Barremian. The top of
159 sequences delivered: *Conorotalites bartensteini bartensteini*, *Glavihedbergella subcretacea*
160 and *Schackoina pustulans* which indicates the late Barremian.

161 d- The Aptian is marked by offshore muds with siliciclastic turbidites (Fig. 3).

162 e- The Jebel Oust late Cretaceous series were studied by Turki (1975) in eastern section of the
163 structure. This section shows that Albian series begins by 60 m thick marly sequences,
164 topped by 180 m platy limestone of uppermost Albian.

165 f- The thinly laminated organic rich 100 m -thick limestones of Bahloul Formation. These series
166 are covered by 450 m-thick of Coniacian Santonian limestone-marls successions topped by
167 150 m-thick Campanian–Maastrichtian Abiod sequences.

2.3. Jebel Kechtilou section

169 The Jebel Kechtilou is a NE-trending faulted anticline. It corresponds to one of numerous structures
170 disturbed during Cretaceous rifting by halokinetic intrusion. Active extensional tectonics have been
171 recorded along the Jebel Kechtilou particularly within Aptian-Albian deposits (Haggui, 2012). The
172 Aptian-Cenomanian series display numerous metric ‘olistostromes’ associated to frequent reworked
173 blocks, slumps, and nodules; all are interpreted as deriving from submarine gravity sliding (Naji et al,
174 2018). The Upper Cretaceous sequences of Jebel Kechtilou have been well described by El Ouardi
175 (1996) and revised in this work (Fig. 4). From the bottom to the top, outcropping Cretaceous series
176 are made of:

177 a- A thick series of ~160 m yellow and yellow-green marls with decametric to metric limestone
178 bed successions. Polygenic conglomerates mark the top of these series, themselves covered
179 by ~120 m of silty green marls topped by 40 cm of breccia layer. These series delivered to
180 Haggui (2012) *Leupoldina pustulans*, *Hastigerinella bizonae* Chevalier, *Ticinella Roberti*
181 (Gandolfi), *Ticinella bejaouensis*, *Ticinella roberti* indicating Aptian age.

182 b- ~120 m bar composed of gray platy limestone beds with ammonites, which were dated as
183 early Albian. This unit is covered by 80 m-thick middle to late Albian deposits consisting of
184 dark gray marls interbedded by gray clayey limestones. They contains an assemblage with
185 *Rotalipora ticinensis*, *Hedbergella breggiensis*. At the top, ~120 m-thick platy limestone bar
186 of was attributed to the uppermost Albian on the basis of *Planomalina buxtorfi* microfauna’s
187 occurrence in thin section (Haggui, 2012).

188 c- Cenomanian sequences show, at the bottom, ~120 m-thick gray limestone bar. The base of
189 sequences contains: *Rotalipora cushmani*, *Rotalipora greenhornensis*, *Hedbergella simplex*,
190 *Hedbergella* sp., *Lenticulina* sp. (Det. Maamouri in El Ouardi, 1996) which indicates the late
191 Cenomanian. The top, of this middle sequences, contains *Whiteinella archaeocretacea*,
192 *Helvetoglobotruncana helvetica*, *Ammodiscus cretaceus*, *Heterohelix* sp. indicating early to
193 middle Turonian age. These series are covered by ~90 m gray marls with gray decametric to
194 metric limestone succession beds which was dated as late Turonian based on microfaunal
195 association with *Marginotruncana schneegansi*, *Marginotruncana pseudolinneiana*,
196 *Hedbergella flandrini*.

197 d- ~180 m-thick series made of monotone marl-limestone successions topped by metric rich-
198 Inocerames limestone beds. The samples collected from the upper part of this series

199 delivered a Coniacian association consisting of *Dicarinella primitiva*, *Dicarinella concavata*,
1 200 *Marginotruncana schneegansi*, *Marginotruncana praeconcavata*, *Hedbergella flandrini*,
2 201 *Lenticulina rotulata*.

3 202 e- ~900 m-thick gray flaky marls with a micropaleontological association including *Sigalia*
4 203 *carpatica* (Det. Zaghbib-Turki and Rami in [El Ouardi, 1996](#)) attesting a Santonian age. The
5 204 Santonian marls are covered by ~220 m gray marls with white to gray clayey limestone beds,
6 205 dated as early Campanian with *Globotruncana elevata* fauna. The Campanian sequences are
7 206 followed by ~140 m white limestone beds alternated with marly joints, dated as middle to
8 207 upper Campanian containing *Globotruncana ventricosa* and *Globotruncanita stuartiformis*.

15 208 **2.4. Jebel Rihane section**

16 209 The Jebel Rihane corresponds to a WNW-to NW-trending syncline ([Ben Yagoub, 1978](#)). It is located
17 210 eastern of Jebel Oust structure and it is mainly made up of Upper Cretaceous deposits. This structure
18 211 exposes Cretaceous series ranging from Aptian to Maastrichtian. Ages are deduced from [Florida](#)
19 212 [\(1963\)](#) and [Ben Yagoub \(1978\)](#) works, which they indicate that the Jebel Kechtilou section shows
20 213 reduced thickness with a comparable microfaunal assemblage. The Jebel Rihane clearly exposes
21 214 considerable thickness variation of Aptian-Albian sequences suggesting a local basin configuration.
22 215 This configuration reflects a tilted blocks geometry produced by the reactivation of inherited faults
23 216 ([Naji et al., 2018](#)).

24 217 **2.5. Medjez-El-Bab sections**

25 218 The Medjez-El-Bab area exposes early Cretaceous sequences in the Jebel El Mourra, Jebel Bou Rahal
26 219 and Sidi Mohamed Akermi localities with significant thicknesses changes ranging from tens meters to
27 220 hundreds of meters ([Fig. 5](#)).

28 221 **2.5.1. Jebel El Mourra**

29 222 The Jebel El Mourra is a NE-trending anticline structure consists by Triassic and reduced early
30 223 Cretaceous series. It was subject to various interpretations as a salt dome structure by [El Ouardi](#)
31 224 [\(1996\)](#) or as a single salt sheet extruded during the Cretaceous forming a submarine salt glacier by
32 225 [Masrouhi and Koyi \(2012\)](#). The Cretaceous series plunging above Triassic rocks are as follow:

33 226 a- 20 m of decametric platy limestones beds separated by marly joints. This first unit delivered:
34 227 *Planomalina buxtorfi* GANDOLFI, *Rotlipora appenninica* MORROW, *Hedbergella*
35 228 *planispira* TAPPAN, *H. delrioensis* CARSEY (Det. Zaghbib-Turki and Rami in [El Ouardi,](#)
36 229 [1996](#)) which allow to attribute it to the uppermost Albian. This latter is covered by an
37 230 observation gap of 15 m-thick.

38 231 b- Marls alternated with metric to decametric limestone beds topped by gray marls. This 55 m-
39 232 thick unit is covered by Plio-Quaternary conglomeratic deposits. Marls delivered to [El Ouardi](#)

233 (1996) the following micro-fauna association *Dicarinella concavata* BROTZEN, *D. primitiva*
234 DALBIEZ, *Marginotruncana undulate* LEHMANN, *M. sinuosa* PORTHAULT , *M.*
235 *tarfayaensis* LEHMANN, *M. pseudolinneiana* PESSAGNO, *Hedbergella flandrini*
236 PORTHAULT, *Lenticulina rotulata* LAMARCK, *Dorothia oxycona* REUSS indicating late
237 Coniacian age. The upper marls delivered *Marginotruncana pseudolinneiana* PESSAGNO, *M.*
238 *undulate* LEHMANN, *M. tarfayaensis* LEHMANN indicative of Santonian age.

239 Masrouhi and Koyi (2012) described a coral algal reef on the upper Albian marls dated by
240 *Planomalina buxtorfi*. The Cenomanian sequences were characterized by the occurrence of
241 *Globotruncana appenica*, and, the Turonian limestones by the presence of
242 *helvetoglobotruncana Helvetica*. The Coniacian–Santonian delivered *Globotruncana coronata* and
243 *Dicarinella concavata* in the bottom and *Dicarinella concavata assymetrica* in the top.

244 2.5.2. Jebel Bou Rahal section

245 Jebel Bou Rahal is a NE-trending south-East dip limb of Medjez-El-Bab anticline structure and
246 shows an interbedded Triassic salt sheet with early Cretaceous sequences. According to El
247 Ouardi, (1996) Cretaceous series (Fig. 5) shows from the bottom to the top:

- 248 a- A first unit is formed by ~160 m green clays with limestone and sandstone beds successions in
249 which limestone beds predominate to the top. This unit is attributed to upper Barremian-Aptian
250 age by correlation of lithological units of nearby sections.
- 251 b- A second unit showing at the base ~80 m green marls and scarce gray decametric clayey
252 limestone beds, followed by ~40 m-thick gray limestone bar, itself covered by 35 m-thick marls
253 with ammonites-rich flaky limestones sequences. This unit is topped by ~25 m-thick gray platy
254 limestone bar covered by ~25 cm-thick yellow siltstone sequences. The platy limestone unit
255 contains: *Planomalina buxtorfi*, *Hedbergella simplex*, *Hedebergella planispira*, *Hedebergella*
256 *delrioensis*, *Rotalipora appenninica* (Det. Zaghib-Turki and Rami in El Ouardi, 1996),
257 characterizing the uppermost Albian. The Lower part of this series delivered *Tincinella roberti*,
258 *Tincinella bejaouaensis*, *Hedebergella infracretacea*, *Nodosaria prismatica*, *Nodosaria nuda*,
259 *Ramulina* sp., *Dentalina linearis*, *Lenticulina muensteri* (Det. Salaj in El Ouardi, 1996) which attest
260 the early Albian. The middle bar of flaky limestone delivered to El Ouardi (1996) the following
261 association *Tincinella bejaouaensis*, *Tincinella roberti*, *Dentalina* sp., *Lenticulina* sp. which
262 indicates early to middle Albian age.
- 263 c- The platy limestones unit is covered by ~4 m-thick bar consists of limestone breccia that resides
264 monogenic conglomerates. This unit is attributed to Cenomanian-Turonian age.
- 265 d- Marls with Metric to decametric limestone beds successions. Marls delivered *Dicarinella*
266 *concavata*, *Dicarinella primitiva*, *Marginotruncana sinuosa*, *Marginotruncana pseudolinneina*,

267 *Globotruncana angusticarinata* (Det. Salaj and Rami in [El Ouardi, 1996](#)) which attests the late
1 268 Coniacian age.

3 269 e- The last unit is covered by an observation gap of 250 m-thick then an outcrop of ~120 m-thick
4 gray marls topped by Nummulitic limestone beds of the early Eocene. These marls delivered
5 270 *Dicarinella asymetrica*, *Dicarinella concavata*, *Marginotruncana tarfayaensis*, *Marginotruncana*
6 271 *sinuosa*, *Sigalia carpatica* and *Dorothia oxycona* (Det. Zaghib-Turki and Rami in [El Ouardi, 1996](#))
7 272 which indicate the Santonian.
8
9 273

12 274 **2.5.3. Jebel Bou Rahal to Sidi Mohamed Akermi section**

14 275 The Jebel Bou Rahal locality exhibits thick Cretaceous sequences ranging in age from Barremian to
15 Coniacian ([Fig. 5](#)). According to [El Ouardi \(1996\)](#), from the base to the top, this section exposes:

16 276
17
18 277 a- ~80 m of gray to dark marls with thin-bedded sandstone layers and gray bioclastic limestone
19 beds intercalations. These successions are covered by ~60 m-thick carbonate unit made of
20 278 three limestone bars topped by platy gray to black limestone beds with Ammonites. The first
21 279 bar exposes reworking blocks with the same facies. The top of this first unit is formed by ~40
22 280 m of silt and sandy marls with gray sandy limestone layers. This first unit was dated as late
23 281 Barremian age, on the basis of rich microfauna association ([El Ouardi, 1996](#)).
24
25 282

26
27 283 b- ~120 m-thick green marls sequences containing iron and celesto-barite nodules with metric
28 and decimetric gray limestone beds characterized by belemnites and breccia. This series are
29 284 covered by 50 cm-thick polygenic conglomerate unit. these were dated as Bedoulian-
30 285 Gargasian on the basis of the following association: *Lingulogavenillela sigmoicosta*
31 286 *barremiana*, *Epistomina carpeuleri*, *Hedbergella infracreteceas*, *Hedbergella tuschepsensis*,
32 287 *Hedbergella bolli*, *Hedbergella* sp., *Leupoldina pustulans*, *Leupoldina protuberans*, *Dentalina*
33 288 *nana*, *Dentalina* sp., *Lenticulina roemeri*, *Lenticulina* sp., *Ortokarstenia senestralis*,
34 289 *Ammodiscus tenuissimus*, *Vaginulina Arguta*, *Nodosaria* sp. ([El Ouardi, 1996](#)). This sequences
35 290 are covered by 75 m-thick gray flaky marls, themselves topped by 40 cm-thick breccia beds.
36 291 These marls delivered *Planomalina chiniourensis* which mark the late Aptian.
37
38 292

39 293 c- ~200 m-thick green marls with numerous gray decimetric limestone beds successions
40 294 characterized by slump folds and septaria ([Masrouhi and Koyi, 2012](#)) followed by an
41 295 observation gap of 60 m , and then 120 m-thick gray platy limestone bar. These rich
42 296 ammonite limestone beds are surmounted by 170 m-thick marls with limestone
43 297 intercalations. The lower successions part and the lower part of platy limestone bar delivered
44 298 to [El Ouardi, 1996](#) a rich microfauna association including *Tincinella roberti*, *Tincinella*
45 299 *bejaouaensis*, *Haplophragmoides concavus*, *Haplophragmoides nonioninoides*, *Textularia* sp.,
46 300 which indicates the early Albian. The upper marl-limestone alternations indicated a middle
47
48
49
50
51
52
53
54
55
56
57
58
59
60
61
62
63
64
65

301 Albian age attested by *Ticinella primula* (El Ouardi, 1996). These sequences are covered by
1 302 100 m-thick gray rich- ammonites and rudists hard limestone with marls and slumped platy
2
3 303 limestones. This level is dated as uppermost Albian with *planomalina buxtorfi* fauna.

4
5 304 d- ~120 m-thick bar consisting of dark gray laminated limestone beds with abundant
6
7 305 ammonites. These beds show repetitive clayey joints. It was dated as by El Ouardi (1996) on
8
9 306 the basis of the following assemblage: *Rotalipora cushmani*, *Rotalipora greenhornensis*,
10 307 *Hedbergella simplex*, *Wheiteinella archaeocretacea*, *Helvetoglobotruncana helvetica*,
11
12 308 *Ammodiscus cretaceus* which attests the late Cenomanian-early Turonian age. These series
13
14 309 are topped by 90 m marl-limestone alternations. Micropaleontological analysis indicates an
15
16 310 late Turonian age attested by *Helvetoglobotruncana helvetica* disappearance and the
17
18 311 appearance of *Margcinotruncana shneegansi* (Det. Zaghib-Turki and Rami in El Ouardi,
19 312 1996).

20
21 313 e- Large monotone limestone-marl successions dating Coniacian-Santonian age on the base of
22
23 314 the following microfauna association *Globotruncana coronata* and *Dicarinella concavata* at
24
25 315 its bottom and *Pseudolinneiana* sp., *Dicarinella asymetrica* and *D. concavata* at its top
26
27 316 (Masrouhi and Koyi, 2012).

28 317 2.6. Jebel Bechtab section

29
30 318 The Jebel Bechtab, located in southwestern part of the Lansarine belt, is a NNE-trending faulted
31
32 319 anticline, crossed by Triassic evaporitic bodies. This structure is made of Hauterivian-Barremian to
33
34 320 Oligo- Miocene sequences (Masrouhi et al., 2013). The Glib Abiod locality situated in the south-east
35
36 321 of Bechtab structure exposes a reduced late Cretaceous series described by Masrouhi et al. (2013) as
37
38 322 follow:

39 323 a- ~40 m unit formed by dark gray marls with successions of gray platy limestone including
40
41 324 ammonites. This unit delivered *Rotalipora subticinensis*, *R. ticinensis*, *Ticinella breggiensis*,
42
43 325 *Ticinella primula* which indicates the late Albian-to uppermost Albian.

44
45 326 b- ~120 m-thick deposits made up of schistose marls with successions of platy limestone on the
46
47 327 base and metric limestone beds to the top. Middle limestone beds delivered to Masrouhi et
48
49 328 al. (2013): *Rotalipora greenhorensis*, *Rotalipora cushmani*, *Rotalipora reicheli*, and rare
50
51 329 *hedbergellae* which attest the middle to late Cenomanian. The following sequences delivered
52
53 330 rich-filaments and globigerina microfacies with *Rotalipora reichelli*, *Rotalipora cushmani*,
54
55 331 *Dicarinella imbricate*, *Whithenella* sp. which indicates the late Cenomanian-lower Turonian.

56 332 c- ~120 m-thick sequences of black schistose and marl-limestone successions. The middle part
57
58 333 of this series delivered *Dicarinella concavata*, *Dicarinella assymetrica*, *Sigalia carpatica*
59 334 which attest the Santonian age.

335 d- ~60 m-thick chalky limestones sequences of the Campanian–Maastrichtian Abiod Formation.

336 **2.7. Oued Tazega section**

337 Two kilometers to the south, the Cretaceous outcrop of Oued Tazega shows the following litho-
338 stratigraphic succession (Fig. 6):

- 339 a- ~70 m-thick gray marl with siliciclastic intercalations with the following assemblage (Solignac,
340 1927): *Puzosia ligaata d'orb.*, *Holcostephanus astieianus d'orb.*, *Holcosdiscus aff. Incertys*
341 *d'orb.*, *Phylloceras infundibulum d'orb.*, *Duvalia dilatata BLV*, *Belemnopsis pistilliformis* of
342 Valanginien p.p-Hauterivien age. This age attribution was confirmed by Peybernès et al.
343 (1996) as lateral equivalent of the Valanginian-p.p Hauterivian Seroula Formation.
- 344 b- ~150 m thick sequences made of shale, gray marl and limestone alternations. To the top the
345 marly series shows sandstone successions. This unit is dated as Barremian age by its position.
- 346 c- ~200 m-thick sequences of gray marls, alternating with gray limestone beds with clear
347 patina, which delivered rare microfauna i.e. lenticulina and could be attributed to Aptian.

348 **2.8. Jebel Boulahouadjeb section**

349 Jebel Boulahouajeb is a NNE-trending anticline located in the northwestern of Tebourba region. It is
350 part of the large salt structure of Lansarine-Baouala. It exposes thick early Cretaceous sequences as
351 previously described (Solignac, 1927; Zargouni, 1975; Masrouhi et al., 2013) and revised by the
352 present work. This section shows the following lithological succession (Fig. 6):

- 353 a- ~400 m-thick pelitic sequences characterized by the stacking of lenticular sandstone deposit
354 of variable size (from cubic centimeters to blocks of a few cubic meters). The top of this first
355 unit is marked by schistose gray-blue marls, alternating with thin marly limestone beds.
356 These series are attributed to Valanginian-aged Seroula Formation (Khessibi, 1967,
357 Peybernes et al., 1996). The Valanginian-Hauterivian boundary is located in the upper marls-
358 limestone sequences.
- 359 b- ~600 m thick sequences made of schistose gray marl showing intercalations of marly
360 limestones with pyritic Ammonites and Aptychus (Solignac, 1927). The following microfauna
361 association was described: *Lissoceras grasianum d'orb.*, *Phylloceras infundibulum d'orb.*,
362 *Phylloceras semisulcatum d'orb.*, *Holodiscus incertus d'orb.*. Limestone beds provided
363 *Calpionella tintacica*, *Calpionella carpatica* with rare *Hedbergellas* and *Lagenidae* allowing to
364 attribute the base of this set to the Early Hauterivian (dét. Raoult; in Zargouni, 1975). The
365 upper part of these sequences delivered: *Epistomina eichenbergi*, *Spirillina neocomiana*,
366 *Lenticulina ouachensis*, *Dorothia hauterivica*, *Lenticulina gaultina*. Above, studied samples
367 delivered *Epistomina eichenbergi*, *Trochamina sp.*, *Hedbergella planispira*, *Gavelinella sp.*,

- 368 *Lenticulina ouachensis*, *Dorothia hauterivica*, *Lenticulina eichenbergi*, *Vaginulina sp.*
1 attributed to Hauterivian-Barremian age.
2 369
3 370 c- ~100 m-thick hard nodular gray limestones, usually as great benches or platy alternating with
4 schistose gray marl layers containing: *Silisites seranonis d'orb.*, *Paranophites angulicostatus*
5 371 *d'orb.*, *Crioceras angulicostatus* Wolam., *Crioceras barremense* Kil., which allow to attribute
6 372 Barremian age (Solignac, 1927). In thin-section this level shows a micrite with Radiolaire and
7 Hedbergelles. The gray schistose marls enclosing some intercalations of centimetric beds of
8 373 brown quartzites. These sequences are covered by green pelites with sandstone blocks of
9 varied size and rare carbonate intercalations.
10 374
11 375 d- ~400 m-thick sequences delivered spicules of echinoderms associated to *Lenticulina*
12 *eichenbergi*, *Ammobaculites cretaceus*, *Gavelinella barremiana*, *Conorotalites bartensteini-*
13 *intercedens-aptiensis*, *Epistomina ornata*, *Epistomina eichenbergi*, *Trochamina sp.*, of the
14 376 Upper Barremian.
15 377
16 378 e- ~250 m-thick sequence mainly formed by gray schistose marl alternations with marly
17 limestones rich in organic matter beds. This interval constitutes an important reference level
18 379 for correlating the subsidence of deposit areas on the Barremian-Aptian boundary.
19 380
20 381 f- ~120 m-thick sequences of gray marls covered by the quaternary plain of Oued Et tine
21 382 containing *Lenticulina gaultina*, *Conorotalites aptensis*, *Valvulina sp.*, *Ammobaculites*,
22 383 *Dorothia oxycona*, *Dorothia trochus* which indicates Aptian age.
23 384
24 385
25 386
26 387
27 388
28 389
29 390
30 391
31 392
32 393
33 394
34 395
35 396
36 397
37 398
38 399
39 400
40 401
41 402
42 403
43 404
44 405
45 406
46 407
47 408
48 409
49 410
50 411
51 412
52 413
53 414
54 415
55 416
56 417
57 418
58 419
59 420
60 421
61 422
62 423
63 424
64 425
65 426

3. Lithostratigraphic correlation

In the Northern Tunisia, the early Cretaceous sequences has been described as “flyschoid deposits” (Memmi, 1981, 1989; Souquet et al., 1997). The Jebel Oust is considered in northern Tunisia as the type-section of lower Cretaceous. On the basis of Souquet et al. (1997), two 2nd order phases of sequence stacking are distinguished: (1) syn-rift prograding phase controlled essentially by tectonic subsidence and sedimentary infilling extending from late Tithonian to Hauterivian, and, (2) post-rift retrograding/prograding phase driven by transgressive-regressive processes extending from Barremian to Albian.

The Correlation of early Cretaceous measured sections, from northeastern Tunisia, shows a significant facies and thicknesses changes ranging from tens meters to hundreds of meters (Fig. 7). The Sidi-Salem locality situated in the Southeast of the study area exposes a reduced early Cretaceous series (Berriasian-Barremian) compared to Jebel Oust “reference section” where Early Cretaceous series reaches 2000 m of thickness. This variation attests an inconstant sedimentation rate along north Tunisia during early Cretaceous. This local distribution sedimentation was qualified by previous work as the result of the so-called “Zaghouan flexure” (or Zaghouan fault) separating

402 subsiding Jebel Oust area from other edge with reduced thickness (Jebel Sidi-Salem). Apparently, no
1 403 significant flexure has worked at the base of the current Zaghouan fault during the Barremian, but it
2
3 404 is possible to envisage a synsedimentary fault or set of faults further west separating subsiding areas
4
5 405 of the Tunisian trough (Jebel Oust) from other sections with reduced thickness (Turki, 1988; El Khazri
6
7 406 et al., 2013). Further north, in the Medjez-el-Bab area, the Barremian is the old Cretaceous deposits
8
9 407 in outcrop. In this area, Barremian sequences of Jebel Bou Rahal do not exceed 100 m, however 4 km
10
11 408 to the north, the section of Sidi Mohamed Akermi exposes 180 m-thick Barremian deposits (Fig. 5).
12
13 409 To the northwest, in the west of the Lansarine structure, Oued Tazega locality exposes 220 m-thick
14
15 410 Valanginian-Barremian deposits, while the Jebel Boulahouadjeb -which is located two kilometers to
16
17 411 the north- exposes 1500 m-thick sequences for the same period. Consequently, Jebel Boulahouadjeb
18
19 412 is qualified as a significant depocenter with a very high rate of sedimentation. Taking in account the
20
21 413 inherited fault systems controlled this structure, the Boulahouadjeb depocenter is created in
22
23 414 response to an active listric deep normal fault growth and associated to halokinetic movement. The
24
25 415 Cretaceous series of Jebel Boulahouadjeb, reviewed in the present study, reveals strong facies and
26
27 416 thickness similarities with the Jebel Oust "reference" section (Fig. 3). Similarly, Early Cretaceous
28
29 417 series exposes frequent siliciclastic turbidite and reworking metric sandstone blocks of varied size
30
31 418 comparable to those described by Souquet et al. (1997) in Jebel Oust.

32 419 The compilation of the early Cretaceous sequences data conduct to a number of paleogeographic
33
34 420 concerns. The lower Cretaceous sequences, of northeastern Tunisia, show thickness and facies
35
36 421 considerable variation reflecting an irregular sea floor (Fig. 7). The Jebel Boulahouadjeb thick section,
37
38 422 50 km to the northwest of Oust locality, shows strong facies and thickness similarities of Jebel Oust
39
40 423 "type-section". These two sections reflect an active subsidence, which suggest basement faults
41
42 424 activity (probably Zaghouan and Teboursouk faults) under an extensional to transtensional tectonic
43
44 425 regime. Between these two localities, further sections show reduced early Cretaceous sequences. In
45
46 426 details, the 80 Km-long correlation clearly reflects basin infilling very similar to others Tethyan
47
48 427 provinces that are controlled by tilted blocks geometry. In addition, this correlation revealed for the
49
50 428 early Cretaceous, a repetitive depocenters limited and shaped by major synsedimentary listric
51
52 429 normal fault systems.

53 430 The Aptian–Albian ages are perceived to have deposited the thick and rapid sediments rates. The
54
55 431 Aptian-Albian epoch was also characterized by previous studies as the most extreme extensional
56
57 432 period of the south Tethyan margin in North Tunisia (Souquet et al., 1997; Masrouhi et al., 2014b;
58
59 433 Naji et al., 2018).

60 434 After Aptian period, the sandstone deposition is more limited in space, and sedimentation becomes
61
62 435 uniform with homogeneous facies mainly composed of marls and fine-grained limestones. During
63
64
65

436 Albian, a mudstone limestone platform is installed overall the basin. Furthermore, Aptian-Albian
1 437 sediment shows considerable thickness variation but no significant facies variation (sequences are of
2 438 pelagic to hemi-pelagic facies). During this period, Jebel Oust remain a subsident area with a high
3 439 rate of sedimentation. To the West, Jebel Rihane and Jebel Kechtilou structures show also a
4 440 significant thick Aptian-Albian series with thickness that differs from one section to another (Ben
5 441 Yagoub, 1978; El Ouardi, 1996; Haggui, 2012;). In these two localities, numerous Aptian-Albian slump
6 442 folds are associated to further instability features. Sequences are qualified to contain numerous
7 443 features of soft-sediment deformation correlated to the tectonic extension (Naji et al., 2018). From
8 444 Jebel El Mourra to Jebel Bou Rahal (Medjez-El-Bab area) Aptian-Albian series range from 20 m to 225
9 445 m. 4 km to the north, Sidi Mohamed Akermi area exposes 785 m-thick Aptian-Albian deposits. This
10 446 area exposes specifically significant thickness variation of Aptian-Albian sequences (Fig. 5) associated
11 447 to numerous slumps folds, calcareous nodules, breccia and conglomerates which indicates a
12 448 sedimentation operated above an irregular sea floor. Consequently, the distribution of sediments
13 449 was clearly to have been operated under tilted-block geometry tectonic control. The correlation
14 450 highlights also a repetitive high sedimentation rates depocenters separated by area with less rates
15 451 (Fig. 5). Few kilometers southwest of Oued Tazega, a reduced Aptian-Albian sequences are found in
16 452 the Jebel Bechtab structure. In Oued Tazega and Boulahouadjeb structures, only Aptian series are
17 453 correlated, for which thickness strongly varies from ~200 m in Oued Tazega and ~1400 m in Jebel
18 454 Boulahouadjeb, and with abundant synsedimentary features such as slumps folds (Figs. 8, 9), sealed
19 455 normal faults, "olistolith" blocks and breccia (Masrouhi et al., 2013; Naji et al., 2018).
20
21 456 The Correlation of late Cretaceous series shows the same configuration with considerable thickness
22 457 variations, but without facies change (Fig. 8). Since the Cenomanian, the facies heterogeneity
23 458 decreases and all sequences are of pelagic to hemi-pelagic facies. A significant thickening is attested
24 459 in Jebel Oust, Jebel Rihane, Jebel Kechtilou and Sidi Mohamed Akermi which reflects a persisted
25 460 tilted blocks geometry, revealed for the Late Cretaceous, and possibly shaped by major
26 461 synsedimentary normal fault systems (Fig. 9). Coniacian–Santonian deposits seem to seal all the
27 462 above mentioned differentiation and described as post-rift marl-rich sequences (Naji et al., 2018).

48 463 **4. Fault kinematic analysis**

49
50 464 The paleostress regimes are reconstructed based on the analysis of fault slip data populations
51 465 measured in the field at several sites. Brittle deformation is frequently quantified using fault
52 466 kinematic analysis methods. These methods are based on measurements of mesoscale faults and
53 467 associated striation. Sometimes, the observed fault planes have more than one set of striation.
54 468 Distinct families of striae has been separated on the basis of geological field data using relative
55 469 chronology of the striations (crosscutting relationships) and their relations with regional Known
56
57
58
59
60
61
62
63
64
65

470 tectonic events. Fault kinematic analysis commonly determines the reduced stress tensor, i.e. the
471 directions of principal stresses ($\sigma_1 > \sigma_2 > \sigma_3$), and the stress ratio $R = (\sigma_2 - \sigma_3) / (\sigma_1 - \sigma_3)$. Therefore, to support
472 our structural interpretation, more numerous striated fault planes ranging from early to late
473 Cretaceous series are measured and computed. The fault kinematic analysis of mesoscale faults
474 documents a quantitative reconstruction of paleostresses. These paleostresses provide useful
475 information on the compressional, extensional or strike-slip origin of larger structures.

4.1. Early Cretaceous faults

476
477 Early Cretaceous sequences display abundant conglomeratic horizons and slumping, in addition to
478 significant thickness changes (Masrouhi et al., 2013, Gharbi et al., 2015; Naji et al., 2018). The early
479 Cretaceous sequences studied in this work show abundant ~NW, ~NE and ~E-trending centimetric,
480 metric to decametric-scale sealed normal faults. Faults data collected from Early Cretaceous of Jebel
481 Oust and Jebel Sidi-Salem structures are rotated, using fault diagram, to their original orientation to
482 restore their initial tectonic extension. The back-tilted fault diagrams typify a NNW-SSE to NE-SE
483 extensional tectonic regime. Locally, E-trending extension is highlighted.

484 The first three sites show homogenous NNW-trending extensional regime. In details, the first
485 stereoplot (Fig. 10, F13) shows extensional stress regime with a NNW-SSE minimum stress axis (σ_3).
486 These measurements have been done in the Valanginian series of the Jebel Oust's northern limb. The
487 second site is located in Oued Tazega locality. These measurements have been done in the Barremian
488 strata. The stereoplot shows (Fig. 10, F24) typical extensional paleostress regime with NNW-SSE
489 minimum stress axis. The Other fault kinematic data (stereoplot F6 in Fig. 10) collected from Sidi-
490 Salem-Messella structure highlight normal fault populations. This stereoplot provides similar state of
491 paleostress with NNW-SSE local minimum stress axis (σ_3).

492 One stereoplot (Fig. 10, F17) typifies ~N-trending extensional tectonic regime. This latter is calculated
493 from Barremian fault population collected in the same region. Similarly, another stereoplot (Fig. 10,
494 F12) collected from Valanginian sequences of Jebel Oust provides a local NE-trending extensional
495 paleostress tensor.

496 Four back-tilted fault diagrams (F6', F15, F18 and F21, Fig. 10) show a general E-trending extensional
497 tectonic regime with local perturbed direction of σ_3 axis. In details, two measurements (Fig. 10, F6'
498 and F21) have been done in Barremian age strata of Jebel Messella structure and provide E-trending
499 minimum stress axis (σ_3). This different local state of stress could be explained probably by its
500 particular structural setting at the junction of Sidi-Salem-Messella major fault systems. The Third
501 computed paleostress field (Fig.10, F15) shows a pattern of WNW-ESE minimum stress axis (σ_3).
502 These measurements have been done in Hauterivian sequences of Jebel Oust. The back-tilted fault

503 diagrams deduced from fault data collected in Barremian sequences of Jebel Bouala (Fig.10, F18)
1 504 highlights E-W extensional tectonic regime.
2

3 505 **4.2. Aptian-Albian faults**

5 506 An Aptian-Albian unconformity is reported in the whole of Tunisia. The origin of the associated
6 507 deformations is still debated. Several authors assign this unconformity as the result of an extensional
7 508 origin created progressive unconformities of the sedimentary basin-fills (Turki, 1985; Masrouhi and
8 509 Koyi, 2012; Masrouhi et al., 2013). Numerous Aptian-Albian faults are collected from the
9 510 northeastern Tunisian domain. The Aptian Albian deposits seem to be controlled by NW to NE-
10 511 trending major fault systems. The back-tilted Albian fault diagram shows an extensional tectonic
11 512 regime with general NE-SW tectonic extension. This state is significantly homogenous in the entire
12 513 region (Fig. 11).
13
14
15
16
17

18 514 The first paleostress tensor collected from fault populations measured in the Albian sequences of
19 515 Jebel Kechtilou (Fig. 11, F23) typify permanently N-S extensional tectonic regime, which appears that
20 516 prevailed during the entire Albian time. The computed stress tensors belonging to the paleostress
21 517 state of Jebel Sidi-Salem during Aptian-Albian times reveals again a relatively homogenous stress
22 518 field. Two sites (Fig.11, F1 and F16) collected from Albian series provide a tectonic regime with a NE-
23 519 SW tectonic extension. The last site (Fig. 11, F7) situated in Lella Sellalia located in the north-east of
24 520 Lansarine structure shows also a local pattern highlighting a NE-SW minimum stress axis during
25 521 Aptian-Albian period.
26
27
28
29
30
31
32
33

34 522 **4.3. Cenomanian-Turonian faults**

35 523 The most Cenomanian-Turonian striated fault planes indicate that the dominant stress regime in the
36 524 northeastern Tunisia is a WNW-ESE to NW-SE extensional tectonic regime (Fig. 12a). The directions of
37 525 extension computed from fault-slip data sets give a remarkably Cenomanian-Turonian homogeneous
38 526 state of stress in all sites from northeastern Tunisia.
39
40
41
42

43 527 The first paleostress tensor is calculated from Cenomanian-Turonian faults of Jebel Kechtilou
44 528 structure. The stereoplot of this first site (Fig.12a, F19) highlights WNW-ESE extensional tectonic
45 529 regime. The second fault kinematics data (Fig. 12a, F3) collected from Sidi-Salem-Messella structure
46 530 highlight normal fault populations. The stereoplot F3 provides a local NW-SE minimum stress axis
47 531 (σ_3), which confirms the regional paleostress state and permit to relate the regional scale
48 532 deformation to this dated stress regime.
49
50
51
52
53

54 533 The Jebel Bechteb structure (Glib El Abiod area) offers also Cenomanian-Turonian faults populations.
55 534 Most of them are sealed faults and the calculated paleostress tensor is characterized by NW-SE
56 535 minimum stress axis (Fig.12a, F9').
57
58
59

60 536 **4.4. Campanian-Maastrichtian faults**

537 During Campanian-early Maastrichtian times, a regional NNW-SSE to NW-SE extension is
538 documented by the synsedimentary fault populations associated to these sequences (Fig. 12b). This
539 extension is calculated from NNW- and NNE-trending conjugate normal fault systems that cut the
540 Campanian-Maastrichtian carbonates of the Abiod Formation in two localities from northeastern
541 Tunisia, and, all of them are sealed normal faults. The first site is collected from the Abiod Formation
542 of Dar Zoufira locality. The corresponding fault kinematic diagram (Fig.12b, F27) provides a NE-SW
543 extensional tectonic regime. Two additional sites (Fig. 12b, F28 and F29) collected from the lower
544 member of the Abiod Formation of Oued Zitoun locality (northwestern part of Mateur region) show
545 opposite extensional regime. The stereoplots F28 (Fig. 12b) provides NW-SE minimum axis and the
546 stereoplot F29 (Fig. 12b) gives NE-SE minimum axis. This local stress axis perturbation confirms the
547 regional paleostress state and permit to relate the regional scale deformation to this dated stress
548 regime. This later began to change from pure extension to transtensional regime related to the
549 African plate trajectory.

5. Present-day regional geometry of north Tunisia

551 Since the 1980^s, the main crustal structures of North Africa are interpreted as the result of
552 distinguished crustal blocks, which were converged and collided during Alpine Cenozoic period. In
553 that model, different domains are identified on the basis of their lithologic, chronologic and
554 structural affinities (Guiraud, 1998; Roure et al., 2012). In the Atlas region of Tunisia, the belt is
555 classically divided into six major domain i.e. the northern allochthonous Numidian Domain, the
556 northern Atlassic domain, the central Atlassic domain, the southern Atlassic domain, the Saharan
557 platform and the Eastern Sahel and Pelagian domain. Whether the geodynamic interpretation of
558 northern Atlassic domain, authors widely accepted two major fault systems i.e. the Teboursouk
559 thrust fault and the Zaghouan-Ressas thrust fault (Jauzein, 1967; Morgan et al., 1998; De Lamotte et
560 al., 2009; Khomsi et al., 2016). The structural style and the kinematic interpretation suffer from little
561 or non-quantitative documentation on a large scale. Only few works attempt to solve the
562 geometrical reassembly by retracing long structural transects (Rouvier, 1977; Ben Ferjani et al., 1990;
563 Morgan et al., 1998, Khomsi et al., 2009, 2016)

564 In the study area, the Zaghouan-Ressas belt thrust contact is the major northeast-trending fault
565 system, which constitutes the southern edge of a major domain called the Zaghouan unit. This later
566 was defined as T2 by Jauzein, 1967 in its major fault systems enumeration in Tunisia, which was
567 defined 6 major lines numbered from T1 to T6). In the Zaghouna area, this system shows the Jurassic
568 platform limestones thrust over the Cenozoic sequences (Turki et al., 1988; Khomsi et al., 2016).
569 Jurassic sequences are now at 1300 m of elevation, and thus it is believed that they have elevated up
570 at least 2.5 km above their original position. This structural setting is well defined on the basis of

571 lithostratigraphic and structural affinities. Previous studies outlines the implication of the Triassic
1 572 evaporites in the main thrust fault (Turki, 1980; Turki et al., 1988; Khomsi et al., 2016). This fact is
2
3 573 favor to admit that Triassic evaporites are previously concerned by earlier tectonics. It is also clear
4
5 574 that thickness and facies variations characterize the Jurassic and cretaceous sequences early
6
7 575 controlled by active extensional setting (Souquet et al., 1997; Morgan et al., 1998). In thin-skinned
8
9 576 model of deformation, previous studies highlight that such variation guides the style and the position
10
11 577 of the major subsequent thrusting (Turki et al., 1988; Souquet et al., 1997; Morgan et al., 1998).
12
13 578 However, Khomsi et al. (2016) have distinguished two main detachment level: Triassic evaporites and
14
15 579 late Eocene shales. In addition, this work imply the role of reverse basement fault at depth of 2 Km.
16
17 580 This major tectonic unit shows numerous normal faults that are preserved on the major thrust
18
19 581 system. All the above mentioned features are in favor of a system of fault inversion model for the
20
21 582 development of the major Zaghouan thrust system. The Zaghouan unit is limited to the North by
22
23 583 thrust unit called the Teboursouk thrust unit. This front is early defined as major fault system in
24
25 584 north Tunisia (defined as T4 by Jauzein, 1967). This area is characterized by thick Aptian–Albian
26
27 585 sequences and exhibits frequent outcropping salt structures belonging to the northeastern Maghreb
28
29 586 salt province (Masrouhi et al, 2013; Jaillard et al., 2017). In addition, the front of this unit is scattered
30
31 587 by dispersal Jurassic outcropping assigned to upper Tithonian–Berriasian sequences (Peybernes et
32
33 588 al., 1996). Curiously, these sequences are usually inverted when outcrop. Previous studies have been
34
35 589 demonstrated that these series are the deepest deposits of the lower Cretaceous rift (Peybernes et
36
37 590 al., 1996). These pre-configurations are inverted by subsequent shortening events and incorporated
38
39 591 in cleaved zone of folding and thrusting. The present-day configuration highlight at least two major
40
41 592 events of folding. Triassic evaporites are associated to the shortening and the growth of the
42
43 593 structures.

44 594 Cenozoic contractional events resulted in the reactivation of earlier inherited structures, the
45
46 595 development of new faults, and the development of major thrust zones are also well identified in the
47
48 596 far west Algerian basins illustrating equivalent geological field and events, i.e. the Hodna basin and
49
50 597 the Chelif basin (Roure et al., 2012) and Sellaoua basin (for more details see Herkat and Guiraud,
51
52 598 2006). Geologic data document the pre-Neogene inversion of former depocenters in the Saharan
53
54 599 Atlas in Algeria (Roure et al., 2012). Previous studies documented some of the Mesozoic normal
55
56 600 faults directly extend into the crystalline basement, whereas others become listric at depth and root
57
58 601 along Triassic evaporites. Many of them have been reactivated as reverse faults, or passively rotated
59
60 602 in fold and thrust structures during subsequent compression. In Algerian basins, lateral thickness
61
62 603 variations within the Jurassic and Cretaceous series are shown, which reflect the south Tethyan
63
64 604 passive margin basins developed during Mesozoic times.

605 Field relationships between units and the present distribution of faults and folds clearly involve the
606 role of the inherited structures in the growth and the style of north Tunisia fold-and-thrust belt.
607 Halokinetic structures developed during Mesozoic rifting, led to the implication of the Triassic
608 evaporites in major thrust systems.

609 **6. Discussion**

610 During Mesozoic times, the North African domain pertain to the Southern Tethyan rifted continental
611 margin. The rift stage, started during Permian (?)–Triassic, is followed during Jurassic and Cretaceous
612 times by passive margin basin’s style (Tlig, 2015; Martín-Martín et al., 2017; Moragas et al., 2017).
613 The correlation of 10 sections studied from the northeastern Tunisia, on the base of new
614 stratigraphic precisions together with existent data from previous works, shows a considerable
615 thickness and facies variations of Cretaceous series reflecting clear tilted-blocks geometry. The early
616 Cretaceous series in northern Tunisia, showing significant thicknesses variation, reflecting that they
617 were deposited above an irregular sea floor. The abundant synsedimentary features (slumps, sealed
618 normal faults, syntectonics conglomerates, lenticular sandstone blocks...) testify for Mesozoic
619 extensional tectonic regime and display character of related growth strata (Masrouhi et al., 2013,
620 2014a; Naji et al., 2018). Based on this study and previous paleogeographic reconstruction’s data
621 (e.g. Souquet et al., 1997; Soua, 2016), the early Cretaceous sequences of the Tunisian Atlas can be
622 subdivided into four second order cycles. The first two cycles extending from late Tithonian to
623 Hauterivian are included within the rifting phase where basement block-faulting predominates
624 (creating regional tilted blocks geometry). Third and fourth cycles extend from the Barremian to
625 Albian can be integrated within a geological setting related to the intra-basin growth faulting. The
626 Jebel Oust Section is considered as the type-section of lower Cretaceous in northern Tunisia (Ben
627 Ferjani et al., 1990; Souquet et al., 1997), where 2600 m-thick siliciclastic and marly sequences have
628 been deposited. The present study demonstrates that an equivalent to this “reference” section is
629 even found 50 km to the north. Therefore, taking in account the current stratigraphic precisions, the
630 1700 m-thick Jebel Boulahouadjeb section may be also undertaken as a representative section
631 equivalent to “reference” section in northern Tunisia where the early Cretaceous is thick and
632 fossiliferous (Fig. 3). Moreover, during early Cretaceous times, these two localities (Jebel
633 Boulahouadjeb and Jebel Oust) seem to be two significant subsident depocenters with a high rate of
634 sedimentation, created in response to active normal faulting. Similarly, the reworked blocks and soft-
635 sediment deformations observed until late Barremian determines the existence of listric active faults
636 controlling the Cretaceous sedimentation of northeastern Tunisia domain. The fault kinematic
637 analysis highlights a NNW to NE extensional regime during early Cretaceous, showing local E-W
638 extensional regime.

639 The Aptian–Albian ages are perceived to have the most extreme extensional related-structures time
1 640 of the south Tethyan edge in North Tunisia (Souquet et al., 1997; Masrouhi et al., 2014b). These data
2
3 641 are well correlated on regional scale in term of subsidence, for which recent studies were established
4
5 642 subsidence curves from the central high Atlas of Morocco to eastern Tunisia (Moragas et al., 2018).
6
7 643 The lower cretaceous period is recognized as the period of rapid subsidence in northern Tunisia and
8
9 644 accompanied by active salt movement. The studied sections show significant thickness variation of
10
11 645 Aptian-Albian deposits accompanied with numerous slump folds (Masrouhi et al., 2013; Naji et al.,
12
13 646 2018) which indicates clearly a contemporaneous submarine slope in the regional context of the
14
15 647 Southern Tethyan rifted continental margin that operates in an extensional regime with tilted blocks
16
17 648 geometry. This instability indicates a synsedimentary listric normal fault systems activity in a context
18
19 649 of an extensional paleomargin.

20 650 Since the Cenomanian, the facies heterogeneity decreases. The homogeneity of the late Cretaceous
21
22 651 facies reflects a basin post-rifting subsidence history. The back-tilted fault diagrams show WNW to
23
24 652 NW-trending extension during Cenomanian time. Coniacian–Santonian deposits seem to seal all the
25
26 653 aforementioned differentiation and can be qualified as post-rift marl-rich sequences followed by
27
28 654 limestone and marl sequences approximately homogeneous in the entire basin (Fig. 13). During
29
30 655 Campanian-Maastrichtian times, a regional NW-trending extension is documented, in which Upper
31
32 656 Cretaceous tectonic was related to a general North Africa extensional paleomargin, at least until
33
34 657 earliest Maastrichtian time (Masrouhi et al., 2008; Gharbi et al., 2013).

35
36 658 In addition to the above-mentioned criteria, the normal faulting at depth actively controls Triassic
37
38 659 salt movements. The Aptian-Albian times were reported as the maximum period of salt structure
39
40 660 growth in northern Tunisia (Masrouhi et al., 2013; Jaillard et al., 2017). The evolution of salt
41
42 661 structures are related to fault-controlled depocenters that occur and were observed along all the
43
44 662 Atlasic margin from Morocco (Moragas et al., 2018) to Tunisia (Jaillard et al., 2017). The tilted block
45
46 663 systems is associated to salt evacuation and then the creation of mini-basins in local fault blocks (Fig.
47
48 664 13).

49 665 **7. Conclusion**

50 666 Detailed lithostratigraphic surveys, long sequence correlations, faults kinematic analysis together
51
52 667 with existent data of relationship tectonic-sedimentation allow us to constrain the structural
53
54 668 architecture and the deformational style of the Cretaceous basin in northern Tunisia as basin with a
55
56 669 sedimentation patterns preferentially guided by tilted blocks geometry. The main conclusions are as
57
58 670 follows:

- 59 671 • Significant facies and thickness variations are deduced along the northeastern Atlas of
60 672 Tunisia,

673
1
2 674
3
4 675
5
6 676
7
8 677
9
10 678
11 679
12
13 680
14
15
16
17
18
19
20
21
22
23
24
25
26
27
28
29
30
31
32
33
34
35
36
37
38
39
40
41
42
43
44
45
46
47
48
49
50
51
52
53
54
55
56
57
58
59
60
61
62
63
64
65

- N-S to NE-SW extensional tectonic regime prevailed during early Cretaceous, and, WNW-ESE to NW-SE extension during late Cretaceous,
- The normal faulting is associated to repetitive local depocenters with a high rate of sedimentation as well as abundant syntectonic conglomeratic horizons and slump folds, and
- The tilted block system is associated to salt evacuation and then the creation of mini-basins in local fault blocks.

681 **References**

- 1
2 682 Ben Ferjani, A., Buroillet, P. F., Mejri, F., 1990. Petroleum Geology of Tunisia. ETAP publication, 194p.
3
4 683 Ben Haj Ali, M., Jedoui, Y., Dali, T., Ben Salem, H., Memmi, L., 1987. Geologic Map of Tunisia
5
6 684 1:500.000. National Office of Mines, National Geological Survey, Tunisia.
7
8 685 Ben Yagoub, J., 1978. Etude géologique de la région de Bou Arada (Atlas tunisien). PhD thesis (Thèse
9
10 686 3ème cycle), Pierre-et-Marie-Curie University (Paris VI), 91 p.
11
12 687 Boughdiri, M., Cordey, F., Sallouhi, H., Maalaoui, K., Masrouhi, A., Soussi, M., 2007. Jurassic
13
14 688 radiolarian-bearing series of Tunisia: biostratigraphy and significance to western Tethys correlations.
15
16 689 Swiss J. Geosciences., 100, 431–441.
17
18 690 Buroillet, P.F., 1956. Contribution à l'étude stratigraphique de la Tunisie centrale. Ann. Mines. Géol.
19
20 691 Tunisie 18, 352 p, Tunis.
21
22 692 Chihaoui, A., Jaillard, E., Latil, J. L., Zghal, I., Susperregui, A. S., Touir, J., Ouali, J., 2010. Stratigraphy of
23
24 693 the Hameima and lower Fahdene Formations in the Tadjerouine area (Northern Tunisia). Journal of
25
26 694 African Earth Sciences, 58, 387–399.
27
28 695 De Lamotte, D.F., Leturmy, P., Missenard, Y., Khomsi, S., Ruiz, G., Saddiqi, O., Guillocheau, F.,
29
30 696 Michard, A., 2009. Mesozoic and Cenozoic vertical movements in the Atlas system (Algeria, Morocco,
31
32 697 Tunisia): An overview. Tectonophysics, 475, 1, 9-28.
33
34 698 Dhahri, F., Boukadi, N., 2010. The evolution of pre-existing structures during the tectonic inversion
35
36 699 process of the Atlas chain of Tunisia. Journal of African Earth Sciences, 56, 139–149.
37
38 700 Dhahri, F., Boukadi, N., 2017. Triassic salt sheets of Mezzouna, Central Tunisia: New comments on
39
40 701 Late Cretaceous halokinesis and geodynamic evolution of the northern African margin. Journal of
41
42 702 African Earth Sciences, 129, 318–329.
43
44 703 El Amari, E.A., Gharbi, M., Youssef, M.B., Masrouhi, A., 2016. The structural style of the Southern
45
46 704 Atlassic foreland in Northern Chotts Range in Tunisia: field data from Bir Oum Ali Structure. Arab J
47
48 705 Geosci 9:389
49
50 706 El Ouardi, H., 1996. Halocinèse et rôle des décrochements dans l'évolution géodynamique de la
51
52 707 partie médiane de la zone des dômes. PhD thesis, University of Tunis II, Tunis.
53
54 708 Elkhazri, A., Abdallah, H., Razgallah, S., Moullade, M., Kuhnt, W., 2013. Carbon-isotope and
55
56 709 microfaunal stratigraphy bounding the Lower Aptian Oceanic Anoxic Event 1a in northeastern
57
58 710 Tunisia. Cretaceous Research, 39, 133–148.
59
60 711 Elkhazri, A., Razgallah, S., Abdallah, H., Ben Haj Ali, N., 2009. The Barremo-Aptian anoxic event « OAE
61
62 712 1a » in northeastern Tunisia: Interest of foraminifers. Revue de Paléobiologie, Genève, 28 (1), 93-130.
63
64
65

713 Florida, S., 1963. Contribution à l'étude géologique de Jebal Rihane. Dipl. Ing. Géol. Ecole Nat. Sup.
1 714 du pétrole, Paris.
2
3 715 Gharbi, M., Espurt, N., Masrouhi, A., Bellier, O., Amari, E. A., 2015. Style of Atlassic tectonic
4 716 deformation and geodynamic evolution of the southern Tethyan margin, Tunisia. *Marine Petroleum*
5 717 *Geologie*, 66, 801–816.
6
7 718 Gharbi, M., Masrouhi, A., Espurt, N., Bellier, O., Amari, E., Ben Youssef, M., Ghanmi, M., 2013. New
8 719 tectono-sedimentary evidences for Aptian to Santonian extension of the Cretaceous rifting in the
9 720 Northern Chotts range (Southern Tunisia). *Journal of African Earth Sciences*, 79, 58–73.
10
11 721 Guiraud, R., Bosworth, W., 1997. Senonian basin inversion and rejuvenation of rifting in Africa and
12 722 Arabia: synthesis and implications to plate-scale tectonics. *Tectonophysics*, 282, 39–82.
13
14 723 Guiraud, R., 1998. Mesozoic rifting and basin inversion along the northern African Tethyan margin:
15 724 an overview. In: MacGregor, D.S., Moody, R.T.J., Clark-Lowes, D.D. (Eds.), *Petroleum Geology of*
16 725 *North Africa*. Geological Society, London, Special Publication, 133, 217–229.
17
18 726 Haggui, M., 2012. Mécanismes de l'halocinèse de la structure salifère du Jebel Kechtilou (monts de
19 727 Testour, Tunisie du nord) : comparaison et modèle. Master's Thesis, University of Sfax, p 73.
20
21 728 Herkat, A., Guiraud, R., 2006. The relationships between tectonics and sedimentation in the Late
22 729 Cretaceous series of the eastern Atlasic Domain (Algeria). *Journal of African Earth Sciences*, 46,
23 730 346–370.
24
25 731 Jaillard, E., Bouillin, J. P., Ouali, J., Dumont, T., Latil, J. L., Chihaoui, A., 2017. Albian salt-tectonics in
26 732 Central Tunisia: Evidences for an Atlantic-type passive margin. *Journal of African Earth Sciences*, 135,
27 733 220–234.
28
29 734 Jaillard, E., Dumont, T., Ouali, J., Bouillin, J. P., Chihaoui, A., Latil, J. L., Arnaud, H., Arnaud-Vanneau,
30 735 A., Zghal, I., 2013. The Albian tectonic "crisis" in Central Tunisia: Nature and chronology of the
31 736 deformations. *Journal of African Earth Sciences*, 85, 75–86.
32
33 737 Jauzein, A. 1967 Contribution à l'étude géologique des confins de la dorsale tunisienne (Tunisie
34 738 Septentrionale). *Ann Mines Géol Tunis*, 22, 1–475.
35
36 739 Khessibi, M., 1967. Etude stratigraphique et structurale des formations mésozoïques de Djedeida-
37 740 Beauvoir (Tunisie), Geol. High study diploma. University of Tunis, 80p.
38
39 741 Khomsi, S., de Lamotte, D.F., Bédir, M., Echihi, O., 2016. The Late Eocene and Late Miocene fronts of
40 742 the Atlas Belt in eastern Maghreb: integration in the geodynamic evolution of the Mediterranean
41 743 Domain. *Arabian Journal of Geosciences*, 9, 15, art. No. 650.
42
43 744 Khomsi, S., Ben Jemia, M.G., Frizon de Lamotte, D., Maherssi, C., Echihi, O., Mezni, R., 2009. An
44 745 overview of the Late Cretaceous-Eocene positive inversions and Oligo-Miocene subsidence events in

746 the foreland of the Tunisian Atlas: structural style and implications for the tectonic agenda of the
1 747 Maghrebian Atlas system. *Tectonophysics* 475, 38–58.
2
3 748 Maamouri, A. L. and Salaj, J., 1978. Les Ventilabrellinae et les Pseudotextulariinae, deux nouveaux
4 taxons de ta famille Heterohelicidae Cushman, 1927 emend. *Annales de, Mines et de la Ggéologie* 28
5 749 (Actes VI Coll. Afric. Micropaléont.), 103-109.
6
7 750
8
9 751 Martín-Martín, J.D., Vergés, J., Saura, E., Moragas, M., Messager, G., Baqués, V., Razin, P., Grélaud,
10 C., Malaval, M., Jousiaume, R., Casciello, E., Cruz-Orosa, I., Hunt, D.W., 2017. Diapiric growth within
11 752 an Early Jurassic rift basin: The Tazoult salt wall (central High Atlas, Morocco). *Tectonics*, 36, 1, 2-32.
12
13 753 Masrouhi, A., Koyi, H. A., 2012. Submarine ‘salt glacier’ of Northern Tunisia, a case of Triassic salt
14 754 mobility in North African Cretaceous passive margin. Geological Society, London, Special Publications,
15 755 363, 579-593.
16
17 756
18
19 757 Masrouhi, A., 2006. Les appareils salifères des régions de Mateur-Tébourba et Medjez-El-Bab (Tunisie
20 758 du Nord). PhD thesis, University of Tunis II, Tunis.
21
22 759 Masrouhi, A., Bellier, O., Ben Youssef, M., Koyi, H., 2014a. Submarine allochthonous salt sheets:
23 760 gravity-driven deformation of North African Cretaceous passive margin in Tunisia - Bled Dogra case
24 761 study and nearby salt structures. *J. Afr. Earth Sci.* 97,125–142.
25
26 762 Masrouhi, A., Bellier, O., Koyi, H., 2014b. Geometry and structural evolution of Lorbeus diapir,
27 763 northwestern Tunisia: polyphase diapirism of the North African inverted passive margin. *Int J Earth*
28 764 *Sci (Geol Rundsch)* 103:881–900.
29
30 765 Masrouhi, A., Bellier, O., Koyi, H., Vila, J. M., Ghanmi, M., 2013. The evolution of the Lansarine–
31 766 Baouala salt canopy in the North African Cretaceous passive margin in Tunisia. *Geological magazine*,
32 767 150, 5, 835–861.
33
34 768 Masrouhi, A., Ghanmi, M., Ben Slama, M.M., Ben Youssef, M., Vila, J.M., Zargouni, F., 2008. New
35 769 tectono-sedimentary evidence constraining the timing of the positive tectonic inversion and the
36 770 Eocene Atlasic phase in northern Tunisia: implication for the North African paleo-margin evolution.
37 771 *Comptes Rendus Geoscience* 340, 771–778.
38
39 772 Mattoussi Kort, H., Gasquet, D., Ikenne, M., Laridhi Ouazaa, N., 2009. Cretaceous crustal thinning in
40 773 North Africa: Implications for magmatic and thermal events in the Eastern Tunisian margin and the
41 774 Pelagic Sea. *Journal of African Earth Sciences*, 55, 5, 257–264.
42
43 775 Memmi L., 1981. Biostratigraphie du Crétacé inférieur de la Tunisie Nord-Orientale. *Bull. Soc. Géol.*
44 776 *France.*, (7), t XXIII, n°2, 157-183.
45
46 777 Memmi L., 1989. Le Crétacé inférieur (Berriasien-Aptien) de Tunisie. *Biostratigraphie,*
47 778 *Paléogéographie et Paléoenvironnements.* Thèse Sci.Univ. Lyon I.157 p. inédite.
48
49
50
51
52
53
54
55
56
57
58
59
60
61
62
63
64
65

779 Moragas, M., Vergés, J., Nalpas, T., Saura, E., Martín-Martín, J.D., Messenger, G., Hunt, D.W., 2017.
1 780 The impact of syn- and post-extension prograding sedimentation on the development of salt-related
2
3 781 rift basins and their inversion: Clues from analogue modelling. *Marine and Petroleum Geology*, 88,
4
5 782 985-1003.
6
7 783 Moragas, M., Vergés, J., Saura, E., Martín-Martín, J.-D., Messenger, G., Merino-Tomé, Ó., Suárez-Ruiz,
8
9 784 I., Razin, P., Grélaud, C., Malaval, M., Joussiaume, R., Hunt, D.W., 2018. Jurassic rifting to post-rift
10
11 785 subsidence analysis in the Central High Atlas and its relation to salt diapirism. *Basin Research*, 30,
12
13 786 336-362.
14
15 787 Morgan, M. A., Grocott, J., Moody, R. T. J., 1998. The structural evolution of the Zaghouan-Ressas
16
17 788 Structural Belt, northern Tunisia. *Geological Society, London, Special Publication*, 132,405–422.
18
19 789 Naji, C., Gharbi, M., Amri, Z., Masrouhi, A., Bellier, O., 2018. Temporal and spatial changes of the
20
21 790 submarine Cretaceous paleoslope in Northern Tunisia, inferred from Slump folds analysis.
22
23 791 *Proceedings of the Geologists' Association*-In press.
24
25 792 Peybernes, B., Kamoun, F., Durand Delga, M., Thierry, J., Faure, P., Dommergues, J., Villa, J.M., Cugny,
26
27 793 P., Ben Youssef M., 1996. Le jurassique et le Crétacé basal de la Tunisie Nord-Occidentale : essai de
28
29 794 corrélation avec les séries de la Dorsale Tunisienne et de la « ride » Amar-Djédeida. *C. R. Acad. Sci.*,
30
31 795 Paris, 323, 153-162.
32
33 796 Rami, A., 1998. Stratigraphie, micropaléontologie et environnements de dépôt du Crétacé supérieur
34
35 797 de la Tunisie Centro-septentrionale. PhD thesis, University of Tunis II, Tunis, 277 p., 22 pl.
36
37 798 Roure, F., Casero, P., Addoum, B., 2012. Alpine inversion of the North African margin and
38
39 799 delamination of its continental lithosphere. *Tectonics*, 31, 3, TC3006.
40
41 800 Rouvier, H., 1977. Géologie de l'extrême Nord Tunisien: tectoniques et paléogéographies superposés
42
43 801 à l'extrémité orientale de la chaîne Nord Maghrébine. Thèse Sc. Univ. Paris VI, p. 703.
44
45 802 Salignac, M., 1927. Etude géologique de la Tunisie septentrionale.-1 vol., in 8°, Direction générale des
46
47 803 travaux publics (service des mines). 756 p. Imp. J. Barlier, Tunis.
48
49 804 Soua, M. 2016. Cretaceous oceanic anoxic events (OAEs) recorded in the northern margin of Africa as
50
51 805 possible oil and gas shale potential in Tunisia: An overview. *International Geology Review*, 58, 3,
52
53 806 277–320.
54
55 807 Souquet, P., Peybernes, B., Saadi, J., Ben Youssef, M., Ghanmi, M., Zarbout, M., Chikhaoui, M.,
56
57 808 Kamoun, F., 1997. Séquences et cycles d'ordre 2en régime extensif et transtensif: exemple du
58
59 809 Crétacé inférieur de l'Atlas tunisien. *Bull. Soc. Géol. France*, 168, 373–86.
60
61 810 Tlig, S., 2015. The Upper Jurassic and Lower Cretaceous series of southern Tunisia and northwestern
62
63 811 Libya revisited. *Journal of African Earth Sciences*, 110, 100-115.
64
65

- 812 Turki, M. M., 1980. La "faille de Zaghuan" est la résultante des structures superposées (Atlas
1 tunisien centrale). Bulletin de la Société Géologique de France, 7, 3, 321–325.
2
3
4 814 Turki, M. M., 1988. Les inversions tectoniques de la Tunisie centro-septentrionale. Bull. Soc. Géol.
5 France, 8, 3, 399–406.
6
7 816 Turki, M.M., 1975. Etude géologique du Massif Serd-Bargou (Atlas tunisien central). Thèse 3ème
8 cycle, Univ. P. Et M. Curie Paris 5, 85 pp.
9
10 818 Turki, M.M., 1985. Polycinématique et contrôle sédimentaire associée sur la cicatrice Zaghuan-
11 Nebhana. Thèse Doc. Etat, Univ. Tunis et Revue Sc. Terre, C.S.T-I.N.R.S.T, 7, 228 pp.
12
13 819 Zargouni, F., 1975. Etude géologique de la chaîne de Lansarine (Région de Tébourba, Atlas tunisien).
14
15 820 Thèse 3ème cycle, Univ. Pierre-et-Marie-Curie (Paris-VI) ,86p. inéd., Paris.
16
17 821
18
19 822
20
21
22
23
24
25
26
27
28
29
30
31
32
33
34
35
36
37
38
39
40
41
42
43
44
45
46
47
48
49
50
51
52
53
54
55
56
57
58
59
60
61
62
63
64
65

823 **Figures captions**

1 824 **Figure 1.** Simplified geologic map of northern Tunisia (modified from [Bel Haj Ali et al., 1984](#)) with
2
3 825 location of the studied sections in northeastern Tunisia. The inset on the top left shows the location
4
5 826 of Tunisia in North Africa.

6
7 827 **Figure 2.** Detailed lithostratigraphic subdivision of Cretaceous sequences in Jebel Sidi-Salem.

8
9 828 **Figure 3:** NE-SW lithostratigraphic correlation of Early Cretaceous series of Jebel Oust and Jebel
10
11 829 Boulahouadjeb sections.

12
13 830 **Figure 4.** Detailed lithostratigraphic subdivision of Cretaceous sequences in Jebel Kechtilou.

14
15 831 **Figure 5.** NW-SE lithostratigraphic correlation of Cretaceous sequences in Medjez El Beb area (Jebel
16
17 832 El Mourra, Jebel Bou Rahal and Sidi Mohamed Akermi).

18
19 833 **Figure 6.** Detailed lithostratigraphic section of early Cretaceous series in Oued Tazega and the Jebel
20
21 834 Boulahoudjeb. (a), (b) and (c) correspond to lithological units, for detailed description, see in the text.

22
23 835 **Figure 7.** Lithostratigraphic correlation of Cretaceous sequences in Northeastern Tunisia from the
24
25 836 Jebel Sidi Salem (south) to Jebel Boulahouadjeb (north) including the Jebel Oust type-section.

26 837 **Figure 8.** Photographic plate illustrating some important tectono-sedimentary features in the study
27
28 838 area: A) Panoramic view looking to the northwest of the Boulahouadjeb showing thick lower
29
30 839 Cretaceous series. B) Panoramic view showing the contact between Triassic strata of Lansarine
31
32 840 structure and the early Cretaceous sequences in Oued Tazega. C) Panoramic view illustrating
33
34 841 Tempestite deposits in early Cretaceous series of Jebel Sidi-Salem structure. D) Detailed photographic
35
36 842 plate of (C). E) Field photo looking to the North-East showing nodular limestone of the uppermost
37
38 843 Albian outcropping in the northern limb of Jebel Sidi-Salem testifying to a synsedimentary
39
40 844 paleoslope. F) Field photo of sealed synsedimentary early Cretaceous normal fault in the Jebel Sidi-
41
42 845 Salem area. G) Detailed view of photo (F) showing the fault plane. H) and (I) Field photos showing
43
44 846 nodular Aptian-Albian limestone sedimentation (septaria) (black arrows) testifying to a
45
46 847 synsedimentary submarine slope.

46 848 **Figure 9.** Photographic plate illustrating some important tectono-sedimentary features in the study
47
48 849 area: A) Panoramic view looking to the north-east showing Cenomanian-Eocene series of Jebel
49
50 850 Bechtab structure. B) Panoramic view looking to the north showing the thick early Cretaceous series
51
52 851 of Jebel Oust. C) Field photo showing Barremian sandstone slump folds of northern limb of Jebel
53
54 852 Oust testifying sedimentation above an irregular sea floor. D) Syn-tectonic conglomeratic redeposits
55
56 853 in the Albian sequences of Medjez El Beb area. E) Field photo showing slump structures between two
57
58 854 parallel layers (Medjez El Beb structure) testifying to a sedimentation above an irregular sea floor. F)
59
60 855 Small-scale extensive deformation preserved showing a sealed normal fault in the Aptian sequences

856 of Jebel Oust. G) Syn-sedimentary sealed normal fault in the Cenomanian sequences of the southern
1 857 limb of Glib El Abiod structure. H) Small-scale sealed normal fault in the Aptian deposits (M'Cherga
2 formation) of Jebel Oust.
3 858

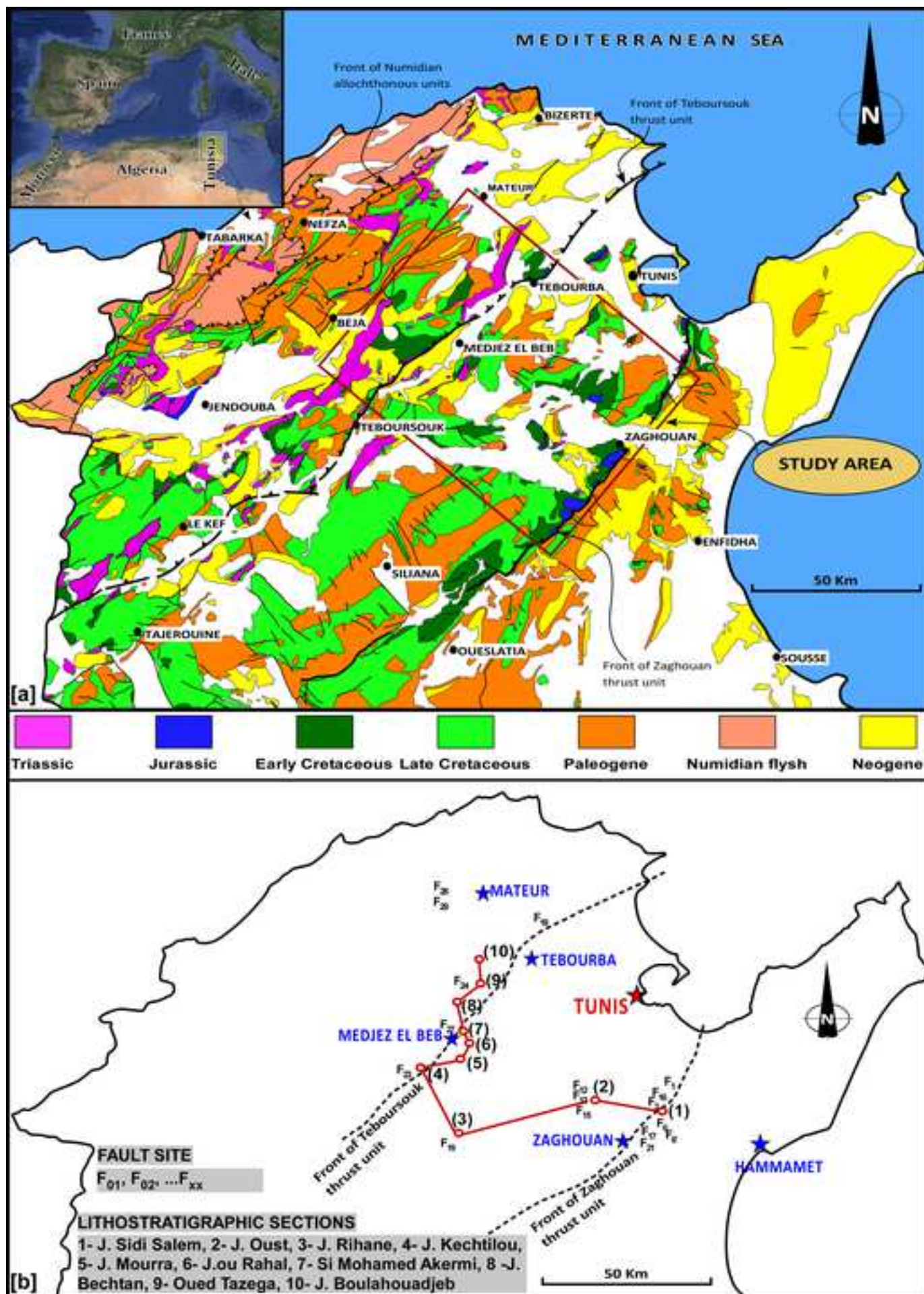
4
5 859 **Figure 10.** Fault kinematic analysis of the synsedimentary early Cretaceous normal faults with lower
6 hemisphere stereograms projection of back-tilted data.
7 860

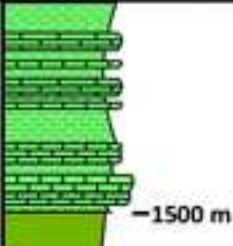
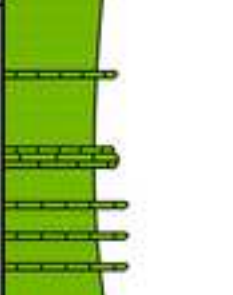


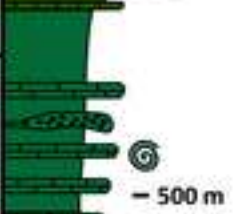


8
9 861 **Figure 11.** Fault kinematic analysis of the synsedimentary Aptian-Albian normal faults with lower
10 hemisphere stereograms projection of back-tilted data.
11 862

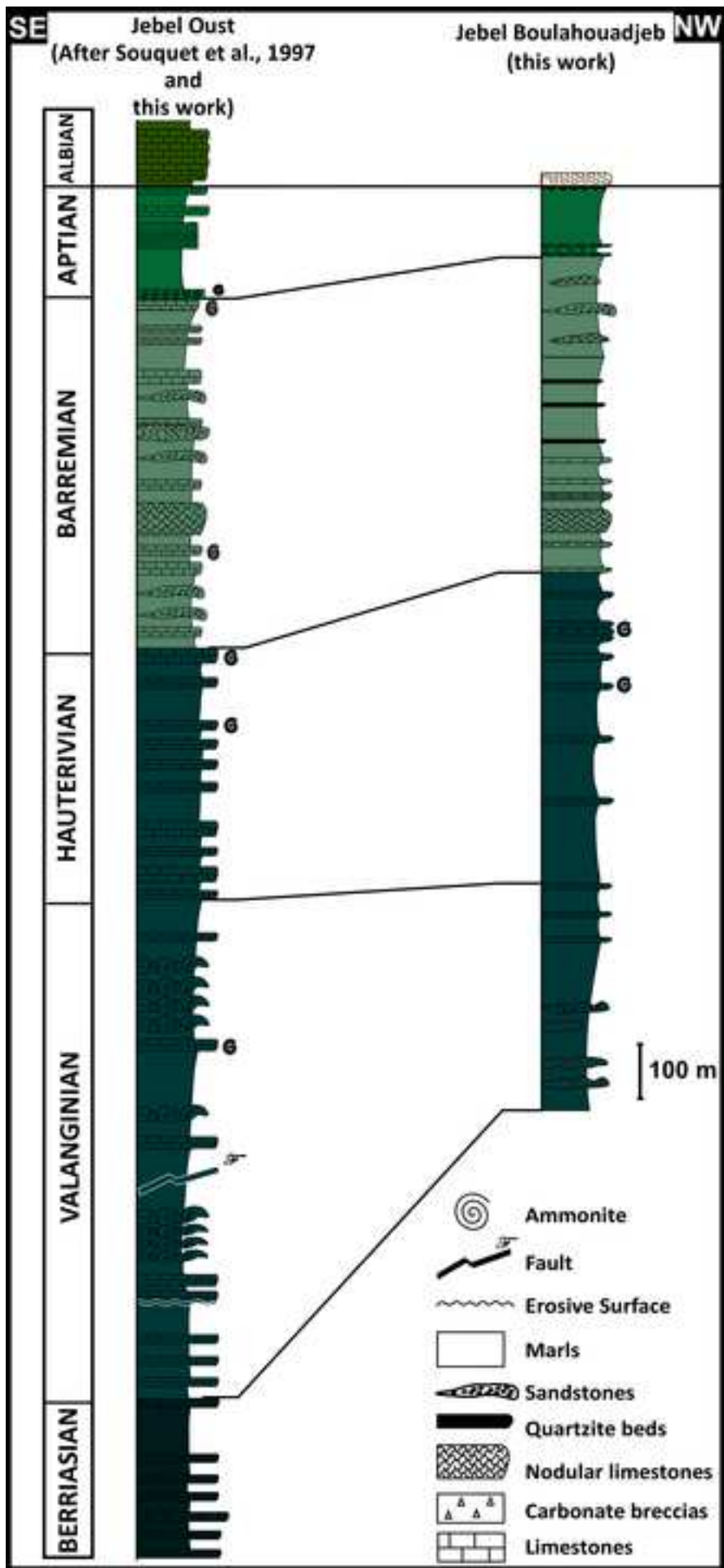
12
13 863 **Figure 12.** Fault kinematic analysis of the synsedimentary late Cretaceous normal faults with lower
14 hemisphere stereograms projection of back-tilted data: (a) During Cenomanian-Turonian times. (b)
15 864 During Campanian-Maastrichtian times.
16 865






17
18 866 **Figure 13.** Simplified reconstructed schematic cross-section (not to scale, in detail this section do not
19 attempt to model the entirely basin's elements) of Northern Tunisia during Cretaceous showing the
20 867 general structural configuration of the basin (based on [Masrouhi et al., 2013, 2014a; Naji et al.,](#)
21 868 [2018](#)).
22 869
23
24 870

25
26 870
27
28
29
30
31
32
33
34
35
36
37
38
39
40
41
42
43
44
45
46
47
48
49
50
51
52
53
54
55
56
57
58
59
60
61
62
63
64
65



Age	Formation	Lithology	Description
CAMPANIAN- MAASTRICHTIAN	Abiod	 -1500 m	White-colored, massive chalky limestone, interbedded with gray marls
CONIACIAN- SANTONIAN	Aleg		Green marls with thin argillaceous limestone beds Limestone interbedded with green marls
CENOMANIAN TURONIAN	Bahloul ?	 -1000 m	Thin dark-gray laminated limestone beds alterned with black-shales
ALBIAN	Fahdene		Metric to centimetric nodular limestone beds interbedded by gray marls. Gray marls intercalated by thin beds of nodular and quartzitic limestone with Ammonites
APTIAN	M'cherga	 - 500 m	Dark to gray laminated marls intercalated with sandstones and dark-gray nodular limestone beds with Ammonites and Belemnites
BARREMIAN			Marls alterned with quartzitic limestone and clayey limestone beds with Ammonites
BERRIASIAN- HAUTERIVIAN	Seroula?	 200 m 0 m	Green to gray marls interbedded by the marly limestone beds



Age	Formation	Lithology	Description
CAMPAIAN MAASTRICHTIAN	Abiod		Decimetric chalky white limestones beds Alternation of gray marl and white gray clayey limestone beds
CONIACIAN-SANTONIAN	Aleg		Monotone gray hard marls series and sometimes flaky marls
CENOZOIC TURONIAN	Bahloul ?		Rich Inocerames limestone beds with gray marls alternations Metric to centimetric limestone beds alterned with gray marls
ALBIAN	Fahdene		Metric limestones beds separated by centimetric joints of marls Gray limestone beds with Ammonites Hard gray marls and platty limestone beds alternations Metric to decimetric laminated limestone beds with Ammonites and sometimes belemnites
APTIAN	Bir M'cherga		Yellow to green flaky marls alterned with decimetric to metric limestone beds topped by polygenic conglomerates

